TITLE: Scaling effects of temperature on parasitism from individuals to host–parasite systems

RUNNING TITLE: Thermal scaling of disease

AUTHORS: Devin Kirk[1,2], Mary I. O'Connor[2], Erin A. Mordecai[1]

AFFILIATIONS:

1. Department of Biology, Stanford University, Stanford, USA.--
2. Department of Zoology, University of British Columbia, Vancouver, Canada.

CONTACT INFORMATION:
Devin Kirk – kirkd@stanford.edu

ABSTRACT

Parasitism is expected to change in a warmer future, but whether warming leads to substantial increases in parasitism remains unclear. Understanding how warming effects on parasitism in individual hosts (e.g., parasite load) translate to effects on population-level parasitism (e.g., prevalence, R_0) remains a major knowledge gap. We analyzed the temperature dependence of parasitism at both host and population levels in thirteen empirical vector-borne host–parasite systems and found a strong, significant positive correlation between the thermal optima of individual- and population-level parasitism. We also found a significant, positive correlation in eleven environmentally-transmitted parasite systems, though several of these systems exhibited thermal optima >5ºC apart between individual and population levels. Similarly, parasitism thermal optima were close to host performance thermal optima in vector-borne systems but not in environmentally-transmitted systems. We then adapted and simulated simple models for both transmission modes and found a similar pattern to the empirical systems: thermal optima in vector-borne systems were more strongly correlated across scales compared to environmentally-transmitted systems. Generally, our results suggest that information on the temperature-dependence, and specifically the thermal optimum, at either the individual- or population-level

should provide a useful—though not quantitatively exact—baseline for predicting temperature dependence at the other level, especially in vector-borne parasite systems. Environmentally-transmitted parasitism may operate by a different set of rules, in which temperature-dependence is decoupled in some systems, requiring the need for trait-based studies of temperature-dependence at individual and population levels.

KEYWORDS: disease, climate change, thermal, scale, transmission, vector-borne, environmentally-transmitted

INTRODUCTION

Climate change is causing organisms to increasingly face temperatures warmer than their optima for physiological performance. These changes in temperature can alter species interactions (Kordas et al., 2011; Thomas and Blanford, 2003), and there is growing evidence that climate change has impacted interactions between individual hosts and their parasites as well as parasite dynamics and outbreaks in host populations (Ben-Horin et al., 2013; Bruno et al., 2007; Claar and Wood, 2020; Harvell et al., 2019; Koelle et al., 2005; Lafferty and Mordecai, 2016; Rohr et al., 2011). Predicting the effects of temperature and changing climate on infectious disease is an urgent priority (Altizer et al., 2013), yet research tends to focus on the level of either an individual host's biology or of host populations, but rarely both.

Understanding how individual-level interactions between hosts and parasites scale to the population level is key for mitigating disease (Fenton, 2008). Indeed, host–parasite interactions span multiple levels of biological organization, from individual cell biology, physiology, and immunology to population dynamics and dispersal among populations, and bridging these levels is an important research area (Handel and Rohani, 2015). Crucially, each of these processes and

the traits that underlie them may be temperature dependent. However, whether the effects of temperature on individual-level parasitism (e.g., on parasite load) typically match the effects of temperature on population-level parasitism (e.g., on parasite prevalence or on the basic reproduction number, R_0) remains an open research gap, as does whether differences in the host–parasite system should affect how thermal effects scale between levels. Understanding the effects of temperature on both individuals and populations is critical for disease prevention and mitigation efforts as the world warms because if the effects are similar across levels of organization, we can leverage observations of the thermal dependence of parasitism at one level to inform predictions in more complex systems. However, if effects of temperature differ across biological scales, using observations on the thermal dependence at one level to extrapolate to the other could provide erroneous predictions for how warming will affect disease in a system.

Beyond exploring how the optimal temperature for parasitism scales across levels, comparing the thermal optima for parasitism to that of the uninfected host can provide a more holistic view of how warming should affect a host–parasite system. One potential framework for doing this is the thermal mismatch hypothesis (Cohen et al., 2017). This hypothesis predicts that parasitism is maximized at temperatures away from the host's optimum—i.e., parasitism peaks at cool temperatures for warm-adapted host species and at warm temperatures for cold-adapted species—at both the host individual and host population levels (Cohen et al., 2019a, 2019b, 2017). Thermal mismatches were first documented in amphibian–chytrid fungus (*Batracochytrium dendrobatidis*, *Bd*) systems at both the individual and population levels (Cohen et al., 2017). More recently, Cohen et al. (2020) analyzed >2000 host–parasite combinations at the population level and found evidence for population-level thermal mismatches: hosts from cool climates had increased disease prevalence at warm temperatures and vice versa. However, outside of amphibian–*Bd* systems, it is unclear whether systems with

thermal mismatches at the population level will also exhibit thermal mismatches at the individual level. How the optimal temperatures for individual- and population-level parasitism compare to the optimal temperature for the host may mediate how climate change will affect host–parasite interactions: decreased host performance at warmer temperatures could either be compounded by increasing parasitism or mitigated by decreased parasitism.

Here, we tested whether there is empirical and theoretical evidence to support the idea that the temperature dependence of parasitism at one level (individuals) approximates temperature dependence at a higher level (populations). First, we surveyed the literature and identified twenty-four systems that report temperature dependence of parasitism at multiple levels. Each system was either vector-borne or environmentally-transmitted, and we hypothesized that thermal optima may scale differently in these two types of systems. We therefore re-analyzed the data separately to test for significant correlations in thermal optima (T_{opt}) across levels in both types of systems. Next, we compared thermal optima of individual- and population-level parasitism to the thermal optimum of host performance in the subset of systems that had information on host performance T_{opt} to test whether the thermal mismatch hypothesis holds across levels in these systems. Finally, we generated and simulated simple temperature-dependent models for vector-borne and environmentally-transmitted parasite systems to test our hypotheses that transmission mode and underlying trait relationships affect how T_{opt} scales. Our findings provide a first step towards finding general rules for how warming temperatures will affect parasitism across biological levels of organization in different types of host–parasite systems.

OVERVIEW OF THERMAL OPTIMA AND PARASITISM

Obtaining, summarizing, and comparing thermal responses across levels of organization can be difficult and sometimes unfeasible. Fortunately, most thermal response curves (TPCs), which project a continuous relationship between a focal trait or process and temperature, have a characteristic non-linear shape with a single optimal temperature at which performance is maximized (the thermal optimum, or T_{opt})(Angilletta, 2006; Huey and Kingsolver, 1989; Huey and Stevenson, 1979). In this study, we therefore focus on and compare thermal optima, as these data are more widely available for many host–parasite systems than full thermal response curves. Though it does not represent the complete thermal response as a TPC would, T_{opt} is a useful metric for comparison both across levels of organization and among taxa because it determines the range of temperatures at which warming has a positive effect on parasitism (for $T < T_{opt}$) versus a negative effect (for $T > T_{opt}$). Other metrics, such as thermal breadth and the minimum and maximum temperatures that allow survival and growth (known as critical thermal minima and maxima), would provide additional information about how climate change could affect host–parasite interactions at the margins of thermal tolerance.

The thermal optima of parasitism could either match or differ across biological levels of organization. First, we may expect a match between optimal temperatures for parasitism at the individual and population levels because processes across the two levels can be linked (Ewald, 1983; Frank, 1996; Handel and Rohani, 2015; Mideo et al., 2011). For example, if the rate-limiting process for population-level parasitism directly depends on a temperature-dependent metabolic rate of the host and/or parasite, then the outcome of individual host–parasite interactions may also depend on temperature (such as if transmission rates scale with individual parasite load (McCallum et al., 2017)) and the effects of temperature on individual-level parasitism may propagate directly to the population level (Anderson and May, 1979). Indeed,

trait-based models have shown that temperature-dependence of underlying traits can cause the basic reproduction number R_0—a key metric in determining if a parasite will or will not cause an epidemic in a host population—to vary with temperature in both vector-borne and environmentally-transmitted parasite systems (Molnár et al., 2013b; Paaijmans et al., 2009; Tesla et al., 2018). From this perspective, the thermal optima of parasitism at the two levels are unlikely to be independent in many systems.

On the other hand, temperature may not have the same effects across levels, even in cases where population-level parasitism is dependent on the dynamics of individual-level parasitism. Indeed, in research on the effects of anti-parasite treatments, models and field experiments have shown that treatment effects on individual hosts do not necessarily lead to equivalent effects in host populations (Fenton, 2013; Nguyen et al., 2021; Pedersen and Antonovics, 2013). The process of parasite transmission among hosts can potentially decouple population dynamics of hosts and parasites from dynamics within host individuals, particularly if the traits that shape the transmission process are temperature dependent (e.g., temperature-dependent activity rate; Casey, 1976). If the thermal optima of traits that affect transmission are much higher or much lower than that of individual-level parasitism, we may expect the thermal optimum of population-level parasitism to be pulled away from the individual-level optimum towards those of transmission-related traits.

One potentially important factor for determining how the temperature-dependence of parasitism scales is the parasite transmission mode. Parasites can be transmitted through the environment, directly (host-to-host), via a vector (a biting arthropod such as a mosquito or tick), or through other modes. Vector-transmitted parasites depend on the vector's ability to successfully transmit the parasite into the host, thereby potentially linking the individual and population levels because parasite growth within the vector can increase the chance of successful

150 transmission (Ohm et al., 2018). Additionally, parasites are often considered to be less virulent
151 within their vectors compared to within their hosts (Wilson et al., 2017), better allowing the
152 parasite to grow within the vector while not greatly diminishing the vector's ability to survive
153 and contact hosts (but see Hu et al., (2008) and Cator et al., (2015) for examples of parasites
154 affecting vector fecundity and behaviour, respectively). By contrast, environmentally-transmitted
155 parasites are not dependent on either a vector or host's ability to contact other hosts. This means
156 that once a parasite is released into the environment, its ability to survive (and in some systems
157 grow and move) will depend only on the parasite propagule's temperature-dependence.
158 Subsequently contacting a new host may separately depend on both temperature-dependent
159 parasite propagule rates and host activity levels. Together, this may lead to a decoupling between
160 the optimal temperature for the parasite within the host (which depends on the interaction
161 between host and parasite temperature-dependence) and population-level transmission and
162 parasitism.
163

164 **RESULTS**

165 ***Empirical systems***

166 The twenty-four empirical systems we analyzed demonstrated a similar range of thermal
167 optima for individual-level parasitism (10.0°C – 29.3°C) and for population-level parasitism
168 (10.0°C – 29.1°C)(Tables 1-2). We found that population-level parasitism T_{opt} was significantly
169 positively correlated with individual-level parasitism in vector-borne systems (Fig. 1a; Pearson
170 correlation = 0.818; 95% CI: 0.486 – 0.944; n = 13). We also found a significant, positive
171 correlation in the environmentally-transmitted systems (Fig. 1b; Pearson correlation = 0.739;
172 95% CI: 0.249 – 0.927; n = 11). Since seven of the eleven environmentally-transmitted systems
173 featured thermal optima that were estimated at the end of temperature range examined in the

study, therefore potentially biasing optima to appear closer to each other than they may be, we also estimated the correlation in the four environmentally-transmitted systems in which both optima were estimated to occur intermediate relative to the temperature extremes examined. This smaller subset of systems showed a non-significant positive correlation (Fig. 1b; Pearson correlation = 0.648; 95% CI: -0.830 – 0.992, n=4).

Ten of thirteen vector-borne systems exhibited thermal optima at individual and population levels that were within 2.5°C of each other (Fig. 1a; Table 1), while only five of eleven environmentally-transmitted systems exhibited optima that were within 2.5°C across levels (Fig. 1b; Table 2). The largest difference across levels appeared in the *Daphnia magna* – *Ordospora colligata* system in which individual-level parasitism peaked at a temperature that is 7°C cooler than the peak for population-level parasitism. Seventeen of the twenty-four systems exhibited thermal optima for population-level parasitism higher or equal to individual-level parasitism, though in most cases this difference was small (Fig. 1; points above the dashed 1:1 line).

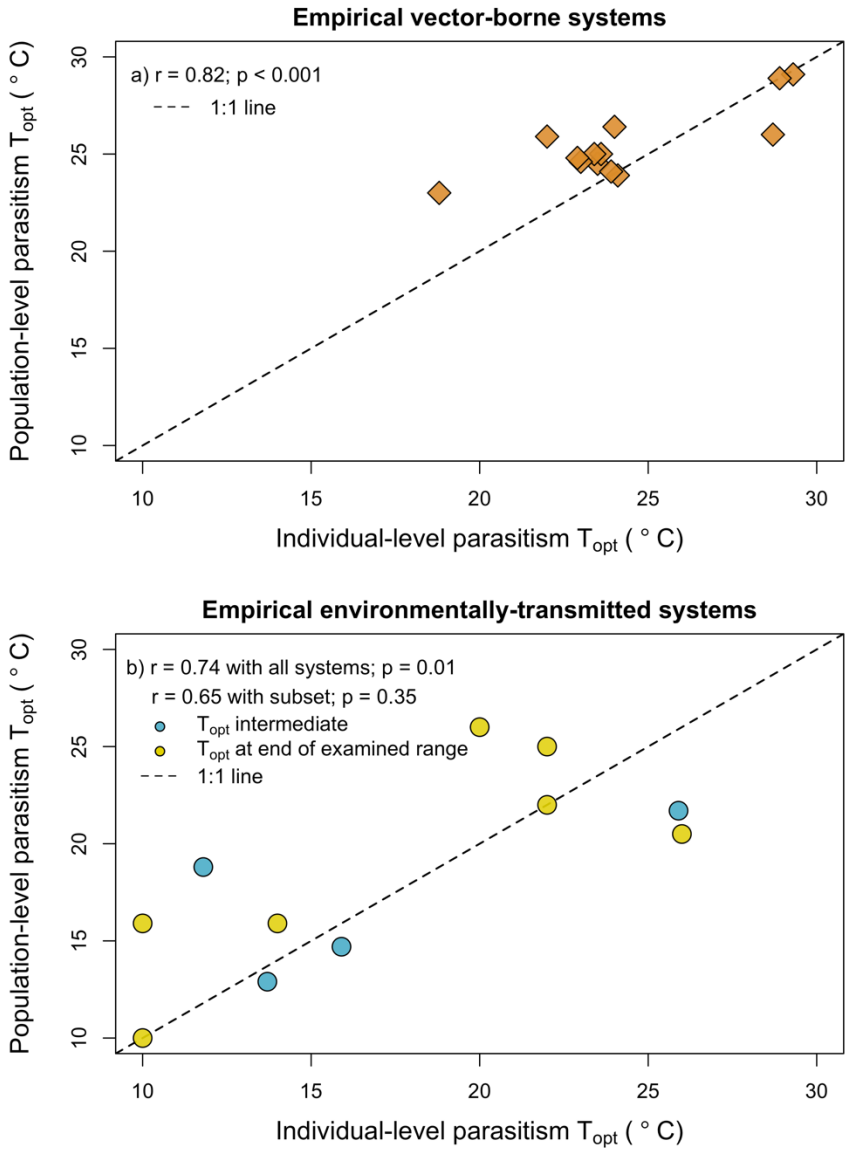

Figure 1. The thermal optima of population-level parasitism are significantly positively correlated with the thermal optima of individual-level parasitism. We found that population-level parasitism T_{opt} was significantly positively correlated with individual-level parasitism T_{opt} in vector-borne systems (a; Pearson correlation = 0.818; 95% CI: 0.486 – 0.944; n = 13) and environmentally-transmitted systems (b; Pearson correlation = 0.739; 95% CI: 0.249 – 0.927; n = 11). The correlation was similar but not significant for the subset of environmentally-transmitted systems that had estimated thermal optima not at the end of their examined temperature range (b; blue circles; Pearson correlation = 0.648; 95% CI: -0.830 – 0.992; n = 4).

Next, we compared the thermal optima of parasitism at both levels to T_{opt} for host performance in the subset of the twenty-four systems that had host performance thermal optima (Fig. 2; n = 17). If a system was situated at the origin in Fig. 2, it would have individual-level parasitism, population-level parasitism, and host performance maximized at the same temperature (i.e., no thermal mismatches exist). Displacement from the origin represents parasitism peaking at temperatures away from where host performance peaks (i.e., thermal mismatches at one or both levels). We found that less than half (7/17) of the systems were situated close to the origin (arbitrarily defined here as within Euclidian distance of 2.5°C, represented by the circle in Fig. 2). However, all seven of these are vector-borne parasite systems, with only two vector-borne systems exhibiting strong thermal mismatches in which both individual-level and population-level parasitism peak at temperatures warmer than host performance (Fig. 2). The remaining ten systems that exhibited thermal mismatches generally supported our hypothesis that if mismatches occurred, they would do so at both levels and in the same direction, as more of these systems were situated in the upper-right or lower-left quadrants of Fig. 2 compared to the upper-left or lower-right quadrants.

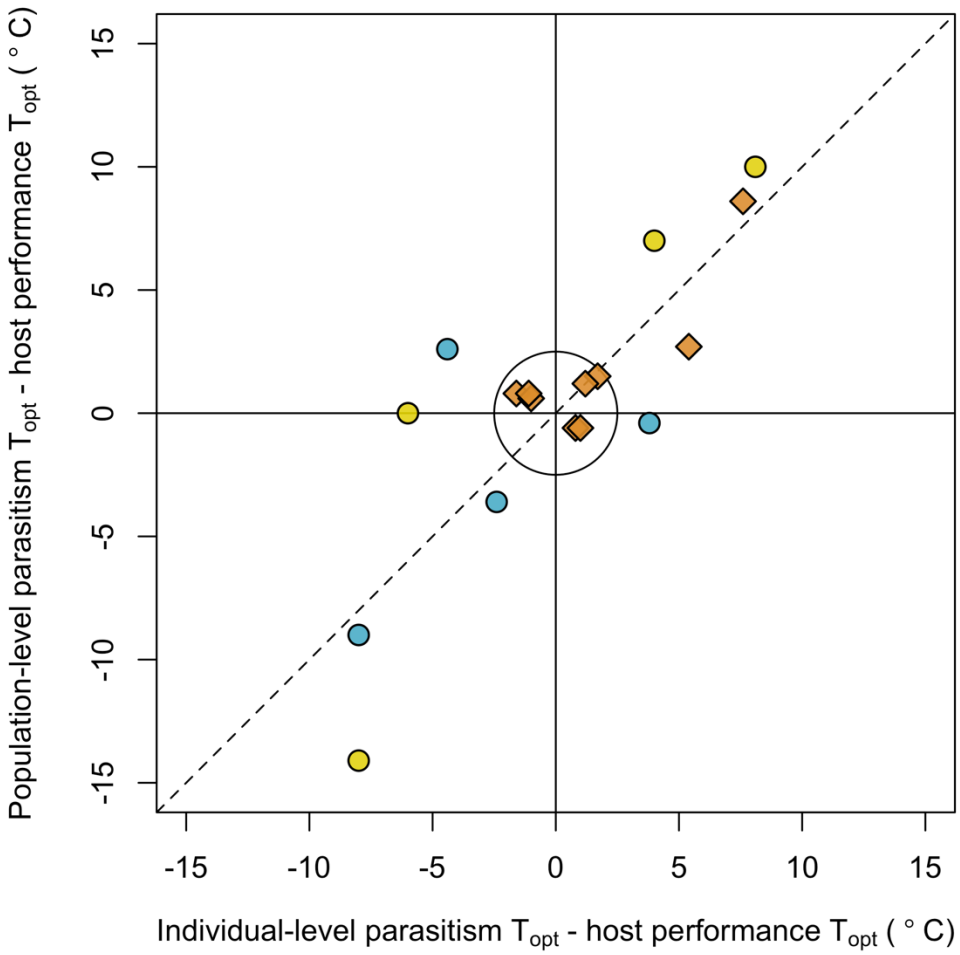

Figure 2. Thermal matches and mismatches tended to be correlated across levels of biological organization. The difference between T_{opt} of population-level parasitism and host performance (y-axis) is plotted against the difference between T_{opt} of individual-level parasitism and host performance (x-axis) for seventeen host–parasite systems. Systems situated at the origin had population-level parasitism, individual-level parasitism, and host performance all maximized at the same temperature (i.e., no thermal mismatches exist), while displacement from the origin represents parasitism peaking at temperatures away from where host performance peaks (i.e., thermal mismatches at individual or population levels). All seven of the systems situated close to the origin (within Euclidian distance of 2.5°C, represented by the black circle) were vector-borne parasite systems (orange diamonds). All environmentally-transmitted systems (blue and yellow circles for systems with parasitism estimated in intermediate range or end of examined range, respectively) exhibited thermal mismatches at one or both levels. Dashed line represents the 1:1 line.

229 ***Simulated systems***

230 We developed and simulated temperature-dependent models to understand how
231 differences in transmission mode or the relationships between traits affect the scaling of T_{opt} at
232 the individual-level (measured as infected days for mosquito-borne systems and parasite load for
233 environmentally-transmitted systems) to the population-level (measured as R_0) for mosquito-
234 borne and environmentally-transmitted parasites. Mirroring the empirical results, the simulated
235 vector-borne parasite systems showed a stronger significant positive correlation between
236 individual- and population-level T_{opt} in system (Fig. 3a; Pearson correlation = 0.681; 95% CI:
237 0.646 - 0.713; n = 1000) compared to any of the three environmentally-transmitted parasite
238 scenarios (Fig. 3b-d). These patterns are qualitatively similar to those found in the empirical
239 systems (Fig. 1), though for both transmission modes, the empirically observed correlations were
240 stronger than those generated in model simulations, which did not assume correlations among the
241 thermal optima for different traits except for those proportional to parasite load. This suggests
242 that organismal constraints on thermal performance across traits in empirical systems may
243 strengthen the correlation between thermal performance of different traits and subsequently of
244 parasitism across multiple scales.

245 The strength of correlation in environmentally-transmitted systems differed significantly
246 depending on the level to which transmission-related processes were dependent on individual-
247 level parasitism. Of the three scenarios, we observed the strongest correlation in host–parasite
248 systems in which both parasite shedding rate and the number of parasites released after host
249 death were proportional to parasite load (Fig. 3b; Pearson correlation = 0.412; 95% CI: 0.359 - 0.
250 462; n = 1000). Systems in which the number of parasites released after host death—but not
251 shedding rate—was proportional to parasite load exhibited a weaker but still significant positive
252 correlation (Fig. 3c; Pearson correlation = 0.257; 95% CI: 0.198 - 0.314; n = 1000). Systems in

253 which neither of these rates or quantities were proportional to parasite load exhibited no
254 correlation in T_{opt} across scales (Fig. 3d; Pearson correlation = 0.003; 95% CI: -0.059 - 0.065), as
255 expected given that this model assumed no correlation in thermal responses among traits and no
256 traits connecting the individual and population scales. These trends were qualitatively similar
257 when we explored different parameter space and model assumptions (Fig. S3-S4).
258
259
260
261

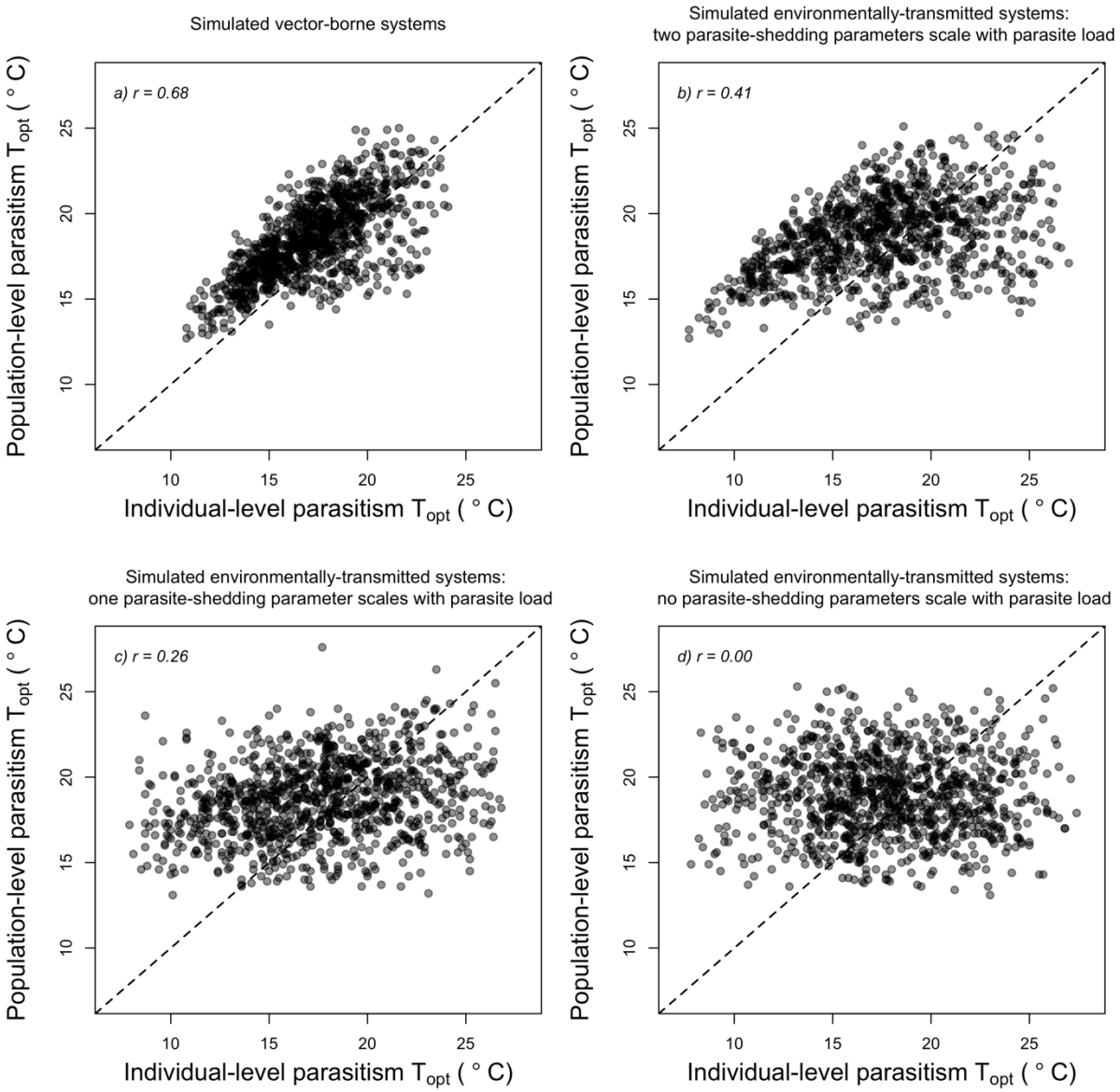

Figure 3. The strength of correlation in simulated systems between thermal optima of individual- and population-level parasitism differs across transmission mode and the level to which transmission-related processes are dependent on individual-level parasitism. Simulated vector-borne parasite systems exhibited a stronger positive correlation (a) than environmentally-transmitted parasite systems (c-d).The strength of correlation in environmentally-transmitted systems differed significantly depending on the number of relationships between individual-level parasitism and transmission-related processes (b-d). Dashed black lines represent the 1:1 lines.

DISCUSSION

To predict how warming temperatures will affect parasites and their hosts, we need to understand how effects of temperature on parasitism scale across levels of biological organization, as well as whether this differs systematically across different types of systems. Moreover, understanding how these effects on parasitism compare to thermal effects on uninfected hosts can offer a more complete view of how climate change will affect host fitness. In our examination of empirical systems, we found a significant positive relationship between parasitism T_{opt} at individual and population levels, though thermal optima tended to be closer at the two scales in vector-borne compared to environmentally-transmitted systems (Fig. 1). Additionally, while individual- and population-level parasitism both peaked at temperatures away from the host optimum in some systems, supporting the thermal mismatch hypothesis, these were primarily environmentally-transmitted, and not vector-transmitted, parasites (Fig. 2), suggesting that thermal mismatches may be more common in certain types of host–parasite systems. Our model also showed how differences in transmission mode and underlying relationships between individual-level parasitism and transmission-related processes can substantially alter the expected relationship between the thermal optima of parasitism in individual hosts and host populations (Fig. 3). Generally, our results suggest that information on the temperature-dependence, and specifically the thermal optimum, at either the individual- or population-level should provide a useful—though not quantitatively exact—baseline for predicting temperature dependence at the other level, though some caution should be taken when extrapolating thermal dependence between levels in environmentally-transmitted parasite systems.

We found a significant positive correlation between T_{opt} of population-level parasitism and T_{opt} of individual-level parasitism, suggesting that the effects of warming on parasitism may

often be in the same direction across levels (Fig. 1). This relationship was strongest in vector-borne systems, likely because temperatures that allow the parasite to best grow within the vector—while not causing it severe damage—will correspond with temperatures where transmission to humans is high. We may intuitively expect environmentally-transmitted systems to exhibit a relationship that is both positive but not as strong as that observed in vector-borne systems, for several reasons. First, we may expect the positive relationship because quantities and rates at the individual level can still correlate with transmission rates in environmentally-transmitted systems, for example the number of parasites shed into the environment can increase with individual parasite load (McCallum et al., 2017). However, once parasites have entered the environment, their survival (and potentially growth and movement) is no longer dependent on the host temperature responses that help determine individual-level parasitism. Instead, the environmental parasite's ability to contact and infect a new host will depend on its own temperature-dependent rates in the environment, potentially its new host's movement or contact rates, and in some cases the parasite's ability to behaviourally thermoregulate (Molnár et al., 2013a). Taken together, for parasites that must travel through the environment rather than transmit via a vector, the temperatures that maximize individual-level parasitism may be decoupled more frequently from those at which transmission within populations peaks.

Population-level parasitism tended to peak at slightly warmer temperatures than individual-level parasitism in the majority of systems (Fig. 1), meaning that these systems may experience small temperature ranges in which warming leads to increases in population-level parasitism but decreases in individual-level parasitism. In the vector-borne systems, this pattern may be because biting rate—a driver of host contact—usually has one of the highest optimal temperatures of all measured traits (Mordecai et al., 2013, 2017, 2019; Shocket et al., 2018a; Villena et al., 2020), thereby shifting R_0 to higher temperatures. A similar process may occur in

environmentally-transmitted systems. It is difficult to definitively parse out the causes of T_{opt} differences in the amphibian–*Bd* systems since individual-level *Bd* parasitism was measured on single frog species in the lab while population-level prevalence by the same parasite was synthesized across many field studies encompassing 235 host species (Cohen et al., 2017; see Materials and Methods for more details). However, the *D. magna–O. colligata* host–microsporidian parasite system can provide an illuminating example, as contact rate in this system is maximized at 30.1°C (Kirk et al., 2019), nearly 20°C warmer than T_{opt} for individual-level parasitism (11.8°C). This is thus a key factor that pulls the thermal optimum of R_0 away from individual-level parasitism T_{opt} to a warmer temperature (18.8°C), illustrating how processes such as contact rate can decouple individual- and population-level temperature dependence. We did not observe any T_{opt} differences this large for vector-borne systems (Table 1, Fig. 1).

The twenty-four systems analyzed here represent only a small slice of the diversity of host–parasite systems that exist. However, some of the trends found in thermal trait biology may be common in other systems, as temperature-dependent metabolic rates are often conserved across systems, and traits can vary accordingly with metabolic rates (Brown et al., 2004; Dell et al., 2011; Molnár et al., 2017). For example, if, as observed in these systems, traits that drive contact across systems (e.g., biting rate, feeding rate, movement rate) tend to exhibit higher thermal optima than traits that determine individual-level parasitism, our finding that population-level parasitism T_{opt} is typically warmer than individual-level parasitism T_{opt} may be common. Further empirical work measuring thermal responses of traits related to parasite transmission in other types of host–parasite systems, such as those with helminth or bacterial parasites—both of which have been shown to be affected by climate (Ben-Haim et al., 2003; Ben-Horin et al., 2013;

Mignatti et al., 2016)—as well as other types of vectors (e.g., ticks, sandflies) and transmission modes will be necessary for determining the generality of this trend.

Our model simulations showed that differences in transmission mode or the level of dependence of transmission-related processes such as parasite shedding rate on individual-level parasitism can affect the scaling of T_{opt}. We found a stronger correlation in vector-borne systems (Fig. 3a) compared to environmentally-transmitted systems (Fig. 3b-d), qualitatively similar to the patterns found in empirical systems (Fig. 1). The quantitative correlations observed were weaker than for the empirical observations, which was not surprising since our models only sought to describe hypothetical vector-borne and environmentally-transmitted host–parasite systems with trait thermal responses drawn at random, ignoring any correlations in thermal responses among traits that are likely to occur in most biological systems. Our model also showed that systems that have more relationships between individual-level parasitism (e.g., parasite load) and processes that affect transmission (e.g., parasite shedding rate) will exhibit stronger scaling of parasitism T_{opt} (Fig. 3b-d). This intuitive result suggests that knowledge of how transmission-related processes do or do not depend on individual-level parasitism in a system can help predict whether the temperature-dependence of parasitism should scale in that system.

The thermal mismatch hypothesis (Cohen et al., 2020, 2019a, 2019b, 2017) has been proposed as an approach for understanding the effects of climate change on host–parasite systems, predicting thermal mismatches in which T_{opt} for parasitism occurs at temperatures away from host T_{opt} due to larger organisms (hosts) generally having narrower thermal breadth than smaller organisms (parasites; Rohr et al., 2018). While empirical evidence shows that thermal mismatches do occur at the population level across many animal systems (Cohen et al., 2020), the novel hypothesis we tested here is that thermal mismatches at the individual level will

correspond with similar thermal mismatches at the population level. Of the eight environmentally-transmitted systems we explored that had T_{opt} data for both host and parasitism at both levels—including the three amphibian–*Bd* systems investigated previously (Cohen et al., 2017)—parasitism tended to peak at temperatures away from the host's optimum in each, meaning that these systems experience thermal mismatches at one or both levels. Our hypothesis was that cold-adapted and warm-adapted hosts experiencing thermal mismatches would fall in the upper-right and lower-left quadrants of Fig. 2, respectively, rather than the upper-left or lower-right, and we found that this was generally the case. As climate change leads to environments warming past the historical temperatures that hosts had previously adapted to, we should expect host systems in the upper-right quadrant to experience the dual threats of both decreased host performance and increased parasitism. In contrast, decreased performance at warmer temperatures for hosts in the lower-left quadrant may be partially offset by decreased parasitism.

Evidence for thermal mismatches occurring at either level was weak in the vector-borne systems. Seven of nine vector-borne systems were situated close to the origin (Fig. 2), suggesting that parasitism and host performance are maximized at close to the same temperatures and that thermal mismatches do not occur at either level. Further, the vector-borne system that showed the most extreme thermal mismatches—*Culex pipiens*–West Nile virus—would likely exhibit smaller thermal mismatches if host traits beyond adult lifespan and fecundity were considered in our host T_{opt} calculation, since larval traits such as larval-to-adult survival and egg viability peak at much warmer temperatures than adult lifespan in this system (Shocket et al., 2020). Notably, when testing for thermal mismatches at the population level, Cohen et al. (2020) also found that thermal mismatch effects were strongest in systems without vectors (or intermediate hosts). Why we observe this pattern will require further investigation in vector-borne systems beyond

391 mosquitos and midges, though it may be related to parasites often causing relatively little harm to
392 their vector (Wilson et al., 2017).

393 To better understand how temperature affects parasitism and to make better predictions
394 for how climate change will affect host–parasite interactions across biological levels, we
395 highlight three important research directions. First, when possible, studies that use experiments
396 to investigate effects of temperature at the individual level can also be used to parameterize
397 simple models of population-level parasitism (a 'bottom-up' approach). Second, field studies
398 investigating population-level parasitism under different climate or weather conditions, often
399 undertaken by measuring the proportion of individuals infected, should also aim to record
400 measures of individual-level parasitism (a 'top-down' approach). The best direct measure would
401 be to record parasite load or an analogous metric measuring the parasite on or within the host,
402 but in cases where this is not possible, indirect measures such as host condition may still be
403 informative. Additionally, collecting contemporaneous information on other environmental
404 factors such as precipitation in terrestrial systems or water quality in aquatic systems will provide
405 necessary insights into how these factors potentially interact with temperature to mediate the
406 thermal optima of parasitism. Finally, studies that document parasitism across an expansive
407 enough temperature range as to estimate temperature thresholds for parasitism—and not only
408 thermal optima—will allow for comparisons across levels that provide insights into the
409 temperatures at which parasitism can be locally extirpated or newly emerge, rather than only
410 increase or decrease. Greatly expanding our repertoire of empirical information on both different
411 host–parasite systems and across wider temperature ranges is critical for understanding the
412 consequences of climate change for human, domestic species, and wildlife disease.

413 Many studies have investigated the effects of temperature on parasitism (reviewed, for
414 example, in Altizer et al., 2013; Claar and Wood, 2020; Lafferty, 2009; Lafferty and Mordecai,

415 2016; Marcogliese, 2008; Rohr et al., 2011), though often at only one of either the individual or
416 population levels. Our findings build upon these studies by emphasizing that how temperature
417 affects individual-level parasitism can scale up to affect parasite transmission, prevalence, and
418 the potential for epidemics in host populations, though not always in a 1:1 manner. More
419 broadly, tying together more theory and empirical results to provide general predictions for how
420 climate change will affect parasitism from individuals to ecosystems in a diverse range of hosts
421 and parasites remains an urgent priority as accelerating climate change makes potentially
422 catastrophic temperature increases of > 2°C increasingly likely by 2050.

423
424
425 **MATERIALS & METHODS**

426 ***Empirical systems***

427 We sought to test hypotheses related to the scaling of thermal optima of both hosts and parasites
428 in empirical systems. We searched the Web of Science using different combinations of search
429 terms such as "temperature", "optima", "parasitism", "parasite development", and "R_0", looking
430 for systems for which measures of individual-level parasitism (e.g., parasite load within or on the
431 host (number of parasites), parasite growth rate on or in the host (days^{-1})), population-level
432 parasitism (e.g., the basic reproduction number R_0, prevalence (infected hosts/total hosts)), and
433 host performance (e.g., lifetime reproduction (offspring)) were estimated across four or more
434 temperatures, allowing us to identify T_{opt} for each of the measures. We identified twenty-four
435 systems for which we were able to identify or calculate parasitism T_{opt} at both levels, seventeen
436 of which also had data to calculate host performance T_{opt}. Thirteen of the systems were vector-
437 borne: eight mosquito–virus systems (Mordecai et al., 2013, 2017; Shocket et al., 2018a, 2020;
438 Tesla et al., 2018), four mosquito–malaria parasite systems (Villena et al., 2020), and one

midge–virus system (El Moustaid et al., 2021)(Table 1). The other eleven systems were environmentally-transmitted: two *Daphnia*–parasite systems (Kirk et al., 2020, 2018; Shocket et al., 2018b), three amphibian–*B. dendrobatidis* (*Bd*, the causative agent of chytridiomycosis) systems (Cohen et al., 2017), a crab–rhizocephalan barnacle parasite system (Gehman et al., 2018), three blue mussel–parasite systems (Galaktionov et al., 2015), and two snail–trematode parasite systems (Nguyen et al., 2021; Paull et al., 2015; Paull and Johnson, 2018)(Table 2). While the mosquito systems are mainly studied with respect to human disease, here we leverage the rich data on their thermal dependence to explore thermal scaling of the mosquito–parasite interaction, which in turn affects transmission to humans and is of major concern for its potential response to climate change (Patz et al., 1995; Zhou et al., 2004). For some systems, thermal optima were estimated based on parameterized trait-based models (e.g., field-validated R_0 models with temperature-dependent parameters), while in others thermal optima were estimated directly from experimental or observational data (Table 2; see Supporting Information for further details). Additionally, uncontrolled environmental factors or different host behaviour could potentially lead to host and parasitism thermal optima differing between the lab and field. However, we did not have enough data to compare reported thermal optima that arose from the lab versus the field, and therefore assume they are equally valid here.

Host performance, individual-level parasitism, and population-level parasitism were measured using different metrics in different systems (Tables 1-2; Supporting Information). We report a single host T_{opt} value for twenty-one of the systems, but two host T_{opt} values (individual and population) for the amphibian systems. This is because individual-level parasitism for three amphibian–*Bd* systems was measured in the lab but the thermal response of population-level parasitism was reported as *Bd* prevalence in the field as a function of environmental temperature for 235 surveyed species, where cold- and warm-adapted amphibians were categorized as those

463 at locations where 50-year mean temperature was <15°C or >20°C, respectively (Cohen et al.,
464 2017). We therefore used separate T_{opt} values for our individual-level host performance
465 (measured as thermal preference in the lab) and population-level host performance (measured as
466 the mean climatic temperature experienced in the field across surveyed species).

467 While we were generally constrained to use whichever metric of parasitism or host
468 performance was reported in each study, we had access to thermal response data for several
469 different metrics in the mosquito–parasite systems. We chose to use the number of infected days
470 as our measure of individual-level parasitism in these systems because it is a composite metric
471 reflecting the effect of temperature on parasite development rate within the mosquito, vector
472 competence (the mosquito's ability to acquire and transmit the parasite), and mosquito survival.
473 We were also interested in how this choice affected our findings of how closely T_{opt} of
474 individual-level parasitism matched T_{opt} of population-level parasitism and T_{opt} of host
475 performance. Generally, using vector competence as a metric of individual-level parasitism gave
476 similar results to our main metric of infected days, but parasite development rate tended to
477 exhibit higher T_{opt} values than the other two metrics (Fig. S3). The Supporting Information
478 contains further details on both our model and the methods used to analyze the empirical
479 systems.

480 We hypothesized that thermal optima in vector-borne systems may scale differently from
481 individual-level parasitism to population-level parasitism compared to thermal optima in
482 environmentally-transmitted systems. We therefore separated the twenty-four systems by
483 transmission mode and tested for a significant correlation in vector-borne systems (n=13) and in
484 environmentally-transmitted systems (n=11) by comparing population-level parasitism T_{opt} to
485 individual-level parasitism T_{opt} using the *cor.test* function in the R package *stats* (R Core Team
486 2021; method = *pearson*). Seven of the environmentally-transmitted systems featured parasitism

T_{opt} at one or two levels that were estimated to occur at either the coldest or warmest temperature examined in the study, potentially biasing T_{opt} estimates to occur closer to each other than would be found if a wider temperature range had been examined. We therefore repeated the correlation test with the subset of environmentally-transmitted systems that had parasitism T_{opt} that were estimated to occur within the limits of the temperatures explored (n=4). In some of the systems, metrics used to calculate individual-level parasitism T_{opt} are also a subset of the metrics used to calculate population-level parasitism T_{opt}. For example, the thermal response of mosquito mortality rate is one of several components used to calculate individual-level parasitism in mosquito–parasite systems, and also one of many components used to calculate population-level parasitism in the same systems. As a result, observed thermal optima for population-level parasitism are not independent from observed thermal optima for individual-level parasitism. While this may affect the interpretation of the observed correlation across systems, we argue that the partial dependence of population-level parasitism on what occurs at the individual-level is biologically realistic for many systems.

Next, using the subset of systems that also had host performance T_{opt} (n=17), we compared T_{opt} for individual- and population-level parasitism to T_{opt} of host performance to determine whether parasitism generally peaked at temperatures away from host thermal optima as predicted by the thermal mismatch hypothesis (Cohen et al., 2019a, 2019b, 2017), whether thermal mismatches at the individual level corresponded to thermal mismatches at the population level, and whether these results were dependent on transmission mode.

Simulated systems

To investigate how different features of a host–parasite system can affect the thermal scaling of parasitism and the observed correlations in T_{opt}, we developed several temperature-

dependent models. This allowed us to link temperature-dependent quantities or processes that occur within individuals (and therefore individual-level parasitism) to a key metric of population-level parasitism (the basic reproduction number, R_0) under different assumptions. Our aim was to investigate whether differences in transmission mode and assumptions regarding trait relationships could result in different patterns in the relationship of thermal optima in parasitism across levels, rather than to exhaustively explore all potential outcomes. As such, these models are not meant to represent specific host–parasite systems, but instead represent a generalized mosquito-borne parasite system and a generalized environmentally-transmitted parasite system under specific thermal biology assumptions.

The temperature-dependent mosquito-borne disease model (Eq. 1) describes how the basic reproduction number, R_0, varies with temperature as a function of several temperature-dependent rates and probabilities. R_0 is a commonly-used metric that represents the number of new infections one infected host should cause in a fully-susceptible population: without stochasticity, $R_0 > 1$ should lead to an epidemic and $R_0 < 1$ should lead to parasite extirpation. Our mosquito-borne model was adapted from a temperature-dependent model for dengue from Mordecai et al. (2017) and similar models have been used to describe R_0 as a function of temperature for malaria and other mosquito-borne diseases (Mordecai et al., 2013; Paaijmans et al., 2009; Shocket et al., 2020; Villena et al., 2020):

$$R_0(T) = \left(\frac{a(T)^2\, bc(T)\, e^{-\mu(T)/PDR(T)}\, EFD(T)\, p_{EA}(T)\, MDR(T)}{N\, r\, \mu(T)^3}\right)^{1/2} \qquad \text{Eq. 1}$$

Here, a is per-mosquito biting rate, bc is vector competence, μ is adult mosquito mortality rate, PDR is parasite development rate, EFD is the number of eggs produced per female per day, p_{EA} is egg-to-adult survival probability, MDR is immature development rate, N is density of humans,

and r is human recovery rate. Following empirical patterns found across mosquito-borne disease systems (reviewed in Mordecai et al., 2019), we modeled biting rate, parasite development rate, eggs production rate, and mosquito development rate using Brière functions (Eq. 2, as described below), and vector competence, egg-to-adult survival probability, and lifespan using concave-down quadratic functions. Mosquito mortality rate μ was set to 1/lifespan.

The Brière function (Eq. 2) is an asymmetrical unimodal function that is often used to describe thermal performance in biological systems (Briere et al., 1999), where c is a positive rate constant, T_{min} and T_{max} are the minimum and maximum temperatures, respectively, T is temperature, and $B(T)$ is set to 0 when $T > T_{max}$ or $T < T_{min}$.

$$B(T) = cT(T - T_{min})(T_{max} - T)^{1/2} \quad \text{Eq. 2}$$

The quadratic function (Eq. 3) is a similarly concave-down function that takes three parameters (positive rate constant c, T_{min} and T_{max}) but is symmetrical rather than asymmetrical.

$$Q(T) = -c(T - T_{min})(T - T_{max}) \quad \text{Eq. 3}$$

To best align with the metrics available from the empirical systems, our metrics for individual-level and population-level parasitism in the mosquito-borne parasite systems are infected days and R_0 (Eq. 1), respectively. Infected days is a function of parasite development rate, vector competence, and mosquito survival (see Supporting Information for additional details on how this is calculated).

We developed the environmentally-transmitted parasite model (Eq. 4) to represent a system in which parasites are shed into the environment throughout the life of an infected host as well as when the host dies. Parasites in the environment can die or infect a susceptible host.

$$R_0(T) = \left(\frac{\chi(T)\,\sigma(T)\,S(T)}{\theta(T)}\right)\left(\frac{\lambda(T)}{\mu(T)+\alpha(T)} + \omega(T)\right)$$

Eq. 4

This modeling approach is commonly used for environmentally-transmitted parasites, and this specific model is similar to a temperature-dependent model developed and empirically validated for the *Daphnia magna – Ordospora colligata* host–parasite system (Kirk et al., 2020).

Here, $\boldsymbol{\chi}$ is *per capita* contact rate between susceptible hosts and parasites in the environment, σ is probability of infection after contact, S is susceptible host density at equilibrium in a disease-free population, θ is parasite mortality rate in the environment, $\boldsymbol{\lambda}$ is parasite shedding rate from an infected host, μ is host background mortality rate, α is host parasite-induced mortality rate, and ω is the number of parasites released into the environment upon host death. To approximate equilibrium susceptible host density (S), we assumed that S is equal to the ratio of host birth rate to background mortality rate. We also assumed that α was proportional to the number of parasites within the host.

We hypothesized that if processes related to environmental parasite transmission were dependent on parasite load within the host, we would observe stronger correlations in T_{opt} across scale. We therefore simulated the environmentally-transmitted model under three different assumptions. First, we assumed that both parasite shedding rate ($\boldsymbol{\lambda}$) and the number of parasites released into the environment upon host death (ω) were each proportional to parasite load (i.e., individual-level parasitism). Next, we assumed that only the number of parasites released after host death (ω) was proportional to parasite load. Finally, we assumed that neither of these rates or quantities were proportional to parasite load.

We modeled the temperature dependence of parasite load (and therefore parasite-induced mortality rate), parasite shedding rate, parasites released after host death, and probability of infection using the quadratic function (Eq. 3), and contact rate and birth rate as Brière functions

(Eq. 2). We modeled the thermal response of background host mortality rate (μ) and parasite mortality in the environment (θ) using concave-up quadratic functions where mortality is minimized at the thermal optimum and increases at cooler and warmer temperatures, as mortality often shows relatively symmetrical responses across temperature (Angilletta, 2009; van der Have, 2002). The thermal response of susceptible host density (S) is a function of the thermal responses of birth rates and background host mortality rates. Our metrics for individual-level and population-level parasitism in the environmentally-transmitted parasite systems are parasite load (Eq. 3) and R_0 (Eq. 4), respectively.

We simulated 1000 mosquito-borne parasite systems and 1000 environmentally-transmitted parasite systems under each of the three assumptions (n = 3000 total) by randomly drawing different thermal response function parameters $\{c, T_{min}, T_{max}\}$ for each temperature-dependent trait in Eqs. 1, 2, 3, and 4. For both Brière and concave-down quadratic functions, T_{min} was drawn from a uniform distribution between 0-10, T_{max} was equal to T_{min} plus a value drawn from a uniform distribution between 15-35, and the rate constant c was drawn from a uniform distribution between 0.5-1.3. Similarly, for the concave-up quadratic function that describes background host mortality rate and parasite mortality rate in the environment in the environmentally-transmitted model (aT^2-bT+c), we drew parameter a from a uniform distribution between 0.0008-0.0009, b from a uniform distribution between 0.02-0.03, and c from a uniform distribution between 0.1-1, and then set baseline host and parasite mortality rates to 0.00667 and 0.0667 (corresponding to max lifespans of 150 days and 15 days), respectively. Thermal responses were scaled to realistic magnitudes for each temperature-dependent trait (e.g., all thermal responses for the contact rate parameter were scaled by a factor of 0.0005). See Supporting Information for more detail, Figs. S1-S2 for examples of the simulated thermal

600 responses, and Figs. S3-S4 for simulations across wider parameter space and varying
601 transmission model assumptions.

602 To test our hypotheses that (1) observed T_{opt} correlations would differ between mosquito-
603 borne (Eq. 1) and environmentally-transmitted parasite systems (Eq. 4), and (2) observed T_{opt}
604 correlations would differ between environmentally-transmitted parasite systems under different
605 trait relationship assumptions, we estimated the correlation between population-level parasitism
606 T_{opt} and individual-level parasitism T_{opt} using the *cor.test* function in the R package *stats* (R Core
607 Team 2021; method = *pearson*) for each of the four cases.

608

609 **ACKNOWLEDGEMENTS**

610 We thank members of the Mordecai and O'Connor labs for valuable feedback on the manuscript.
611 EAM and DK were funded by NIH (R35GM133439); EAM was funded by NSF (DEB-1518681
612 and DEB-2011147, also supported by the Fogarty International Center), a King Center for
613 Global Development seed grant, a Terman Award, and a Center for Innovation in Global Health
614 seed grant.

615 **COMPETING INTERESTS**

616 The authors declare no competing interests.

617

618 **LITERATURE CITED**

619

620 Altizer S, Ostfeld RS, Johnson PTJ, Kutz S, Harvell CD. 2013. Climate Change and Infectious
621 Diseases: From Evidence to a Predictive Framework. *Science* **341**:514–519.
622 doi:10.1126/science.1239401
623 Anderson RM, May RM. 1979. Population biology of infectious diseases: part 1. *Nature*
624 **280**:361–367.
625 Angilletta MJ. 2009. Thermal adaptation: a theoretical and empirical synthesis. Oxford
626 University Press.
627 Angilletta MJ. 2006. Estimating and comparing thermal performance curves. *Journal of Thermal*
628 *Biology* **31**:541–545. doi:10.1016/j.jtherbio.2006.06.002

Ben-Haim Y, Zicherman-Keren M, Rosenberg E. 2003. Temperature-regulated bleaching and lysis of the coral Pocillopora damicornis by the novel pathogen Vibrio coralliilyticus. *AEM* **69**:4236–4242. doi:10.1128/AEM.69.7.4236-4242.2003

Ben-Horin T, Lenihan HS, Lafferty KD. 2013. Variable intertidal temperature explains why disease endangers black abalone. *Ecology* **94**:161–168. doi:10.1890/11-2257.1

Briere J-F, Pracros P, Le Roux A-Y, Pierre J-S. 1999. A Novel Rate Model of Temperature-Dependent Development for Arthropods. *Environ Entomol* **28**:22–29. doi:10.1093/ee/28.1.22

Brown JH, Gillooly JF, Allen AP, Savage VM, West GB. 2004. TOWARD A METABOLIC THEORY OF ECOLOGY. *Ecology* **85**:1771–1789. doi:10.1890/03-9000

Bruno JF, Selig ER, Casey KS, Page CA, Willis BL, Harvell CD, Sweatman H, Melendy AM. 2007. Thermal Stress and Coral Cover as Drivers of Coral Disease Outbreaks. *PLoS Biol* **5**:e124. doi:10.1371/journal.pbio.0050124

Casey TM. 1976. Activity Patterns, Body Temperature and Thermal Ecology in Two Desert Caterpillars (Lepidoptera: Sphingidae). *Ecology* **57**:485–497. doi:10.2307/1936433

Cator LJ, Pietri JE, Murdock CC, Ohm JR, Lewis EE, Read AF, Luckhart S, Thomas MB. 2015. Immune response and insulin signalling alter mosquito feeding behaviour to enhance malaria transmission potential. *Sci Rep* **5**:11947. doi:10.1038/srep11947

Claar DC, Wood CL. 2020. Pulse Heat Stress and Parasitism in a Warming World. *Trends in Ecology & Evolution* **35**:704–715. doi:10.1016/j.tree.2020.04.002

Cohen JM, Civitello DJ, Venesky MD, McMahon TA, Rohr JR. 2019a. An interaction between climate change and infectious disease drove widespread amphibian declines. *Glob Change Biol* **25**:927–937. doi:10.1111/gcb.14489

Cohen JM, McMahon TA, Ramsay C, Roznik EA, Sauer EL, Bessler S, Civitello DJ, Delius BK, Halstead N, Knutie SA, Nguyen KH, Ortega N, Sears B, Venesky MD, Young S, Rohr JR. 2019b. Impacts of thermal mismatches on chytrid fungus Batrachochytrium dendrobatidis prevalence are moderated by life stage, body size, elevation and latitude. *Ecol Lett* **22**:817–825. doi:10.1111/ele.13239

Cohen JM, Sauer EL, Santiago O, Spencer S, Rohr JR. 2020. Divergent impacts of warming weather on wildlife disease risk across climates. *Science* **370**:eabb1702. doi:10.1126/science.abb1702

Cohen JM, Venesky MD, Sauer EL, Civitello DJ, McMahon TA, Roznik EA, Rohr JR. 2017. The thermal mismatch hypothesis explains host susceptibility to an emerging infectious disease. *Ecol Lett* **20**:184–193. doi:10.1111/ele.12720

Dell AI, Pawar S, Savage VM. 2011. Systematic variation in the temperature dependence of physiological and ecological traits. *Proceedings of the National Academy of Sciences* **108**:10591–10596. doi:10.1073/pnas.1015178108

El Moustaid F, Thornton Z, Slamani H, Ryan SJ, Johnson LR. 2021. Predicting temperature-dependent transmission suitability of bluetongue virus in livestock. *Parasites Vectors* **14**:382. doi:10.1186/s13071-021-04826-y

Ewald PW. 1983. Host-Parasite Relations, Vectors, and the Evolution of Disease Severity. *Annu Rev Ecol Syst* **14**:465–485. doi:10.1146/annurev.es.14.110183.002341

Fenton A. 2013. Dances with worms: the ecological and evolutionary impacts of deworming on coinfecting pathogens. *Parasitology* **140**:1119–1132. doi:10.1017/S0031182013000590

Fenton A. 2008. Worms and germs: the population dynamic consequences of microparasite-macroparasite co-infection. *Parasitology* **135**:1545–1560. doi:10.1017/S003118200700025X

Frank SA. 1996. Models of Parasite Virulence. *The Quarterly Review of Biology* **71**:37–78.

Galaktionov KV, Bustnes JO, Bårdsen B-J, Wilson JG, Nikolaev KE, Sukhotin AA, Skírnisson K, Saville DH, Ivanov MV, Regel KV. 2015. Factors influencing the distribution of trematode

larvae in blue mussels Mytilus edulis in the North Atlantic and Arctic Oceans. *Mar Biol* **162**:193–206. doi:10.1007/s00227-014-2586-4

Gehman A-LM, Hall RJ, Byers JE. 2018. Host and parasite thermal ecology jointly determine the effect of climate warming on epidemic dynamics. *Proc Natl Acad Sci USA* **115**:744–749. doi:10.1073/pnas.1705067115

Handel A, Rohani P. 2015. Crossing the scale from within-host infection dynamics to between-host transmission fitness: a discussion of current assumptions and knowledge. *Phil Trans R Soc B* **370**:20140302. doi:10.1098/rstb.2014.0302

Harvell CD, Montecino-Latorre D, Caldwell JM, Burt JM, Bosley K, Keller A, Heron SF, Salomon AK, Lee L, Pontier O, Pattengill-Semmens C, Gaydos JK. 2019. Disease epidemic and a marine heat wave are associated with the continental-scale collapse of a pivotal predator (Pycnopodia helianthoides). *Sci Adv* **5**:eaau7042. doi:10.1126/sciadv.aau7042

Hu C, Rio RVM, Medlock J, Haines LR, Nayduch D, Savage AF, Guz N, Attardo GM, Pearson TW, Galvani AP, Aksoy S. 2008. Infections with Immunogenic Trypanosomes Reduce Tsetse Reproductive Fitness: Potential Impact of Different Parasite Strains on Vector Population Structure. *PLoS Negl Trop Dis* **2**:e192. doi:10.1371/journal.pntd.0000192

Huey RB, Kingsolver JG. 1989. Evolution of thermal sensitivity of ectotherm performance. *Trends in Ecology & Evolution* **4**:131–135.

Huey RB, Stevenson RD. 1979. Integrating Thermal Physiology and Ecology of Ectotherms: A Discussion of Approaches. *American Zoologist* **19**:357–366.

Kirk D, Jones N, Peacock S, Phillips J, Molnár PK, Krkošek M, Luijckx P. 2018. Empirical evidence that metabolic theory describes the temperature dependency of within-host parasite dynamics. *PLoS Biol* **16**:e2004608. doi:10.1371/journal.pbio.2004608

Kirk D, Luijckx P, Jones N, Krichel L, Pencer C, Molnár P, Krkošek M. 2020. Experimental evidence of warming-induced disease emergence and its prediction by a trait-based mechanistic model. *Proc R Soc B* **287**:20201526. doi:10.1098/rspb.2020.1526

Kirk D, Luijckx P, Stanic A, Krkošek M. 2019. Predicting the Thermal and Allometric Dependencies of Disease Transmission via the Metabolic Theory of Ecology. *The American Naturalist* **193**:661–676. doi:10.1086/702846

Koelle K, Pascual M, Yunus M. 2005. Pathogen adaptation to seasonal forcing and climate change. *Proc R Soc B* **272**:971–977. doi:10.1098/rspb.2004.3043

Kordas RL, Harley CDG, O'Connor MI. 2011. Community ecology in a warming world: The influence of temperature on interspecific interactions in marine systems. *Journal of Experimental Marine Biology and Ecology* **400**:218–226. doi:10.1016/j.jembe.2011.02.029

Lafferty KD. 2009. The ecology of climate change and infectious diseases. *Ecology* **90**:888–900. doi:10.1890/08-0079.1

Lafferty KD, Mordecai EA. 2016. The rise and fall of infectious disease in a warmer world. *F1000Res* **5**:2040. doi:10.12688/f1000research.8766.1

Marcogliese DJ. 2008. The impact of climate change on the parasites and infectious diseases of aquatic animals. *Rev scii tech Off init Epiz* **27**:467–484.

McCallum H, Fenton A, Hudson PJ, Lee B, Levick B, Norman R, Perkins SE, Viney M, Wilson AJ, Lello J. 2017. Breaking beta: deconstructing the parasite transmission function. *Phil Trans R Soc B* **372**:20160084. doi:10.1098/rstb.2016.0084

Mideo N, Nelson WA, Reece SE, Bell AS, Read AF, Day T. 2011. Bridging scales in the evolution of infectious disease life histories: application. *Evolution* **65**:3298–3310. doi:10.1111/j.1558-5646.2011.01382.x

Mignatti A, Boag B, Cattadori IM. 2016. Host immunity shapes the impact of climate changes on the dynamics of parasite infections. *Proc Natl Acad Sci USA* **113**:2970–2975. doi:10.1073/pnas.1501193113

Molnár PK, Dobson AP, Kutz SJ. 2013a. Gimme shelter - the relative sensitivity of parasitic nematodes with direct and indirect life cycles to climate change. *Glob Change Biol* **19**:3291–3305. doi:10.1111/gcb.12303

Molnár PK, Kutz SJ, Hoar BM, Dobson AP. 2013b. Metabolic approaches to understanding climate change impacts on seasonal host-macroparasite dynamics. *Ecol Lett* **16**:9–21. doi:10.1111/ele.12022

Molnár PK, Sckrabulis JP, Altman KA, Raffel TR. 2017. Thermal Performance Curves and the Metabolic Theory of Ecology—A Practical Guide to Models and Experiments for Parasitologists. *Journal of Parasitology* **103**:423. doi:10.1645/16-148

Mordecai EA, Caldwell JM, Grossman MK, Lippi CA, Johnson LR, Neira M, Rohr JR, Ryan SJ, Savage V, Shocket MS, Sippy R, Stewart Ibarra AM, Thomas MB, Villena O. 2019. Thermal biology of mosquito-borne disease. *Ecol Lett* **22**:1690–1708. doi:10.1111/ele.13335

Mordecai EA, Cohen JM, Evans MV, Gudapati P, Johnson LR, Lippi CA, Miazgowicz K, Murdock CC, Rohr JR, Ryan SJ, Savage V, Shocket MS, Stewart Ibarra A, Thomas MB, Weikel DP. 2017. Detecting the impact of temperature on transmission of Zika, dengue, and chikungunya using mechanistic models. *PLoS Negl Trop Dis* **11**:e0005568. doi:10.1371/journal.pntd.0005568

Mordecai EA, Paaijmans KP, Johnson LR, Balzer C, Ben-Horin T, de Moor E, McNally A, Pawar S, Ryan SJ, Smith TC, Lafferty KD. 2013. Optimal temperature for malaria transmission is dramatically lower than previously predicted. *Ecol Lett* **16**:22–30. doi:10.1111/ele.12015

Nguyen KH, Boersch-Supan PH, Hartman RB, Mendiola SY, Harwood VJ, Civitello DJ, Rohr JR. 2021. Interventions can shift the thermal optimum for parasitic disease transmission. *Proc Natl Acad Sci USA* **118**:e2017537118. doi:10.1073/pnas.2017537118

Ohm JR, Baldini F, Barreaux P, Lefevre T, Lynch PA, Suh E, Whitehead SA, Thomas MB. 2018. Rethinking the extrinsic incubation period of malaria parasites. *Parasites Vectors* **11**:178. doi:10.1186/s13071-018-2761-4

Paaijmans KP, Read AF, Thomas MB. 2009. Understanding the link between malaria risk and climate. *Proceedings of the National Academy of Sciences* **106**:13844–13849. doi:10.1073/pnas.0903423106

Patz JA, Epstein PR, Burke TH, Balbus JM. 1995. Global Climate Change and Emerging Infectious Diseases. *JAMA: The Journal of the American Medical Association* **275**:217–223.

Paull SH, Johnson PTJ. 2018. How Temperature, Pond-Drying, and Nutrients Influence Parasite Infection and Pathology. *EcoHealth* **15**:396–408. doi:10.1007/s10393-018-1320-y

Paull SH, Raffel TR, LaFonte BE, Johnson PTJ. 2015. How temperature shifts affect parasite production: testing the roles of thermal stress and acclimation. *Funct Ecol* **29**:941–950. doi:10.1111/1365-2435.12401

Pedersen AB, Antonovics J. 2013. Anthelmintic treatment alters the parasite community in a wild mouse host. *Biol Lett* **9**:20130205. doi:10.1098/rsbl.2013.0205

R Core Team. 2021. R: A Language and Environmment for Statistical Computing. https://www.R-project.org/

Rohr JR, Civitello DJ, Cohen JM, Roznik EA, Sinervo B, Dell AI. 2018. The complex drivers of thermal acclimation and breadth in ectotherms. *Ecol Lett* **21**:1425–1439. doi:10.1111/ele.13107

Rohr JR, Dobson AP, Johnson PTJ, Kilpatrick AM, Paull SH, Raffel TR, Ruiz-Moreno D, Thomas MB. 2011. Frontiers in climate change–disease research. *Trends in Ecology & Evolution* **26**:270–277. doi:10.1016/j.tree.2011.03.002

Shocket MS, Ryan SJ, Mordecai EA. 2018a. Temperature explains broad patterns of Ross River virus transmission. *eLife* **7**:e37762. doi:10.7554/eLife.37762

Shocket MS, Strauss AT, Hite JL, Šljivar M, Civitello DJ, Duffy MA, Cáceres CE, Hall SR. 2018b. Temperature Drives Epidemics in a Zooplankton-Fungus Disease System: A Trait-Driven Approach Points to Transmission via Host Foraging. *The American Naturalist* **191**:435–451. doi:10.1086/696096

Shocket MS, Verwillow AB, Numazu MG, Slamani H, Cohen JM, El Moustaid F, Rohr J, Johnson LR, Mordecai EA. 2020. Transmission of West Nile and five other temperate mosquito-borne viruses peaks at temperatures between 23°C and 26°C. *eLife* **9**:e58511. doi:10.7554/eLife.58511

Tesla B, Demakovsky LR, Mordecai EA, Ryan SJ, Bonds MH, Ngonghala CN, Brindley MA, Murdock CC. 2018. Temperature drives Zika virus transmission: evidence from empirical and mathematical models. *Proc R Soc B* **285**:20180795.

Thomas MB, Blanford S. 2003. Thermal biology in insect-parasite interactions. *Trends in Ecology & Evolution* **18**:344–350. doi:10.1016/S0169-5347(03)00069-7

van der Have TM. 2002. A proximate model for thermal tolerance in ectotherms. *Oikos* **98**:141–155. doi:10.1034/j.1600-0706.2002.980115.x

Villena OC, Ryan SJ, Murdock CC, Johnson LR. 2020. Temperature impacts the transmission of malaria parasites by Anopheles gambiae and Anopheles stephensi mosquitoes. *bioRxiv* https://doi.org/10.1101/2020.07.08.194472. doi:10.1101/2020.07.08.194472

Wilson AJ, Morgan ER, Booth M, Norman R, Perkins SE, Hauffe HC, Mideo N, Antonovics J, McCallum H, Fenton A. 2017. What is a vector? *Phil Trans R Soc B* **372**:20160085. doi:10.1098/rstb.2016.0085

Zhou G, Minakawa N, Githeko AK, Yan G. 2004. Association between climate variability and malaria epidemics in the East African highlands. *Proceedings of the National Academy of Sciences* **101**:2375–2380. doi:10.1073/pnas.0308714100

TABLE 1. Thermal optima of parasitism and host performance for thirteen vector-borne host–parasite systems.

Host	Parasite	Individual-level parasitism measure	Population-level parasitism measure	Host performance measure	Individual-level parasitism T_{opt} (°C)	Population-level parasitism T_{opt} (°C)	Host performance T_{opt} (°C)	Data source	Reference
Culex pipiens (mosquito)	West Nile virus	Infected days	R_0	Adult reproduction weighted by lifespan	23.5	24.5	15.9	Experimental	Shocket et al. 2020
Aedes aegypti (mosquito)	dengue virus	Infected days	R_0	Adult reproduction weighted by lifespan	29.3	29.1	27.6	Experimental	Mordecai et al. 2017
Aedes aegypti (mosquito)	Zika virus	Infected days	R_0	Adult reproduction weighted by lifespan	28.9	28.9	27.7	Experimental	Tesla et al. 2018
Culex annulirostris (mosquito)	Ross River virus	Infected days	R_0	Adult reproduction weighted by lifespan	24.0	26.4	25.6	Experimental	Shocket et al. 2018a
Culex tarsalis (mosquito)	Western equine encephalitis virus	Infected days	R_0	NA	18.8	23.0	NA	Experimental	Shocket et al. 2020
Culex tarsalis (mosquito)	West Nile virus	Infected days	R_0	NA	24.1	23.9	NA	Experimental	Shocket et al. 2020
Culex tarsalis (mosquito)	St. Louis encephalitis virus	Infected days	R_0	NA	23.9	24.1	NA	Experimental	Shocket et al. 2020
Aedes taeniorynchus (mosquito)	Rift Valley fever virus	Infected days	R_0	NA	22.0	25.9	NA	Experimental	Shocket et al. 2020
Anopheles gambiae (mosquito)	Plasmodium vivax (apicomplexan)	Infected days	Transmission suitability	Adult reproduction weighted by lifespan	23.6	25.0	24.4	Experimental	Villena et al. 2020
Anopheles gambiae (mosquito)	Plasmodium falciparum (apicomplexan)	Infected days	Transmission suitability	Adult reproduction weighted by lifespan	23.4	25.0	24.4	Experimental	Villena et al. 2020
Anopheles stephensi (mosquito)	Plasmodium vivax (apicomplexan)	Infected days	Transmission suitability	Adult reproduction weighted by lifespan	23.0	24.6	24.0	Experimental	Villena et al. 2020
Anopheles stephensi (mosquito)	Plasmodium falciparum (apicomplexan)	Infected days	Transmission suitability	Adult reproduction weighted by lifespan	22.9	24.8	24.0	Experimental	Villena et al. 2020
Culicoides sp. (midge)	Bluetongue viral disease	Vector competence	Transmission suitability	Population density	28.7	26.0	23.3	Experimental	El Moustaid et al. 2021

↑ R_0 is the basic reproduction number of the parasite in the host population.

TABLE 2. Thermal optima of parasitism and host performance for eleven environmentally-transmitted host–parasite systems.

Host	Parasite	Individual-level parasitism measure	Population-level parasitism measure	Host performance measure	Individual-level parasitism T_{opt} (°C)	Population-level parasitism T_{opt} (°C)	Host performance T_{opt} (°C)	Data source	Reference
Daphnia dentifera (water flea)	Metschnikowia bicuspidata (fungus)	Spore load	R_0	Intrinsic growth rate	20	26*	26*	Experimental	Shocket et al. 2018b
Daphnia magna (water flea)	Ordospora colligata (microsporidian)	Spore load	R_0	Lifetime reproduction	11.8	18.8	16.2	Experimental	Kirk et al. 2018, 2020
Atelopus zeteki (frog)†	Batrachochytrium dendrobatidis (fungus)	Parasite growth rate on host	Prevalence	Thermal preference	26*	20.5	17.9 (10.5)†	Experimental and observational	Cohen et al. 2017
Anaxyrus terrestris (frog)†	Batrachochytrium dendrobatidis (fungus)	Parasite growth rate on host	Prevalence	Thermal preference	10*	15.9	24.1 (23.9)†	Experimental and observational	Cohen et al. 2017
Osteopilus septentrionalis (frog)†	Batrachochytrium dendrobatidis (fungus)	Parasite growth rate on host	Prevalence	Thermal preference	14*	15.9	23 (23.9)†	Experimental and observational	Cohen et al. 2017
Eurypanopeus depressus (crab)	Loxothylacus panopaei (barnacle)	Parasite lifetime reproduction	R_0	Survival	15.9	14.7	18.3	Experimental	Gehman et al. 2018
Biomphalaria spp. (snail)	Schistosoma mansoni (trematode)	Cercarial emergence rate	R_0	Recruitment rate	25.9	21.7	22.1	Experimental	Nguyen et al. 2021
Helisoma trivolvis (snail)	Ribeiroia ondatrae (trematode)	Cercarial release rate	Change in prevalence	Density	22	25*	18*	Experimental and observational	Paull et al. 2015, Paull & Johnson 2018
Mytilus edulis (mussel)	Gymnophallus sp. (trematode)	Parasite intensity	Prevalence	NA	13.7	12.9	NA	Observational	Galaktionov et al. 2015
Mytilus edulis (mussel)	Himasthla sp. (trematode)	Parasite intensity	Prevalence	NA	10*	10*	NA	Observational	Galaktionov et al. 2015
Mytilus edulis (mussel)	Renicola sp. (trematode)	Parasite intensity	Prevalence	NA	22*	22*	NA	Observational	Galaktionov et al. 2015

* T_{opt} for these values was determined at either the warmest or coolest temperature examined in the original study, rather than at a value that was intermediate relative to the range examined.

† Individual-level parasitism and the first number listed for host preference was measured on the single host species. Population-level parasitism and the number in parentheses for host preference was measured across many amphibian species adapted to similar climates. See Materials and Methods for more detail.

↟ R_0 is the basic reproduction number of the parasite in the host population.